3042 J. Phys. Chem. A **1998,** *102,* 3042−3047

Electronic Structure in Pyridinium-Based Metal-to-Ligand Charge-Transfer Excited States by Step-Scan FTIR Time-Resolved Spectroscopy

Pingyun Chen and Richard A. Palmer*

Department of Chemistry, Duke University, Box 90346, Durham, North Carolina 27708-0346

Thomas J. Meyer*

Department of Chemistry, University of North Carolina, Chapel Hill, North Carolina 27599-3290

Received: November 17, 1997; In Final Form: January 28, 1998

Step-scan FTIR time-resolved spectroscopy (S^2FTIR TRS) has been applied to a series of Re^I and Os^{II} polypyridyl complexes that contain *N*-methyl-4,4′-bipyridinium (MQ^+) cation as an electron acceptor. Changes in ν(CO) and ring-stretching vibrations of the acceptor ligands in the fingerprint region provide direct insight into electronic structure both in metal-to-ligand charge transfer (MLCT) excited states and 1-electron reduced complexes. The measurements reveal: (1) changes in metal−ligand back-bonding between the ground and excited state, (2) special characteristics of MQ^+ as an acceptor ligand, including the appearance of an intense ΔA band at $\sim$1610 cm^{-1}, which appears to be vibronically coupled to the internal charge distribution of the reduced ligand, and (3) elucidation of a competition that exists between MQ^+ and 4,4′-$(CO_2Et)_2$bpy as acceptor ligands in *fac*-$[Re(4,4'\text{-}(CO_2Et)_2bpy)(CO)_3(MQ^+)]^{n+}$ ($n = 1, 2$).

Introduction

Time-resolved infrared (TRIR) spectroscopy has emerged as a powerful tool for obtaining structural information on short time scales. Ultrafast TRIR experiments on picosecond (ps) to femtosecond (fs) time scales are typically conducted by pump/probe approaches with short IR pulses generated by frequency mixing or by the upconversion technique pioneered by Hochstrasser et al.[1−5] On the nanosecond (ns) time scale, continuous-wave CO or diode lasers have been used in combination with fast IR detectors.[6] However, these laser-based techniques have a limited spectral range, and the low-energy, “fingerprint” region is not accessible. With the advent of step-scan FTIR spectroscopy, it is now possible to acquire full mid-infrared spectra on the tens of nanoseconds time scale routinely.[7] Coupled with laser flash photolysis this technique has been utilized to explore photochemical ligand loss and protein conformational changes in hemoglobins and myoglobins.[8,9]

The utility of TRIR spectroscopy in inorganic photochemistry has also been demonstrated in applications to metal complexes.[4−7,10−13] Most early studies focused on metal CO- or CN^--containing complexes, for which ν(CO) and ν(CN) bands of high oscillator strengths occur at energies accessible to IR lasers. One of the first examples was the measurement of back electron transfer in the mixed-valence ion $[(CN)_5M^{II}{-}CN{-}M^{III}(NH_3)_5]^-$ (M = Os, Ru) following laser-flash excitation.[13] Shifts in ν(CO) or ν(CN) have also been used to characterize excited states. The ν(CO) bands in the metal-to-ligand charge-transfer (MLCT) excited state(s) of *fac*-$[Re(bpy)(CO)_3Cl]$ are shifted by +44, +73, and +58 cm^{-1} relative to the ground state.[6a,7] For the lowest dppz-localized excited state of *fac*-$[Re(dppz)(CO)_3(PPh_3)]^+$ (dppz = dipyrido[3,2-*a*:2′,2′-*c*]phenazine; PPh_3 = triphenylphosphine), the shift in ν(CO) is <1 cm^{-1}.[10b] Application of step-scan FTIR time-resolved spectroscopy (S^2 FTIR TRS) has allowed transient measurements to be extended to the fingerprint region and used to confirm localization of the excited electron in the lowest MLCT state(s) of $[Ru(bpy^{-\bullet})(bpy)_2]^{2+*}$ on the 100-ns time scale.[11]

In this study, S^2FTIR TRS is applied to the MLCT excited states of the series of Re^I and Os^{II} polypyridyl complexes, *cis*-$[Os(bpy)_2(CO)(MQ^+)]^{3+}$ (bpy = 2,2′-bipyridine; MQ^+ = *N*-methyl-4,4′-bipyridinium cation) and *fac*-$[Re(4,4'\text{-}(CH_3)_2bpy)(CO)_3(MQ^+)]^{2+}$ (X = CH_3, H, CO_2Et) all of which contain the pyridinium acceptor, MQ^+. Ligand structures and their abbreviations are illustrated below.

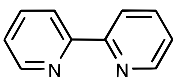

(bpy)

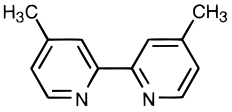

(4,4'-$(CH_3)_2$bpy)

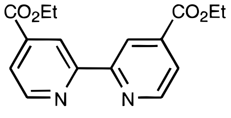

(4,4'-$(CO_2Et)_2$bpy)

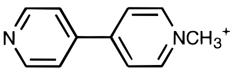

(MQ^+)

In earlier studies on *cis*-$[Os(bpy)_2(CO)(MQ^+)]^{3+}$ and *fac*-$[Re(4,4'\text{-}(CH_3)_2bpy)(CO)_3(MQ^+)]^{2+}$, time-resolved measurements demonstrated that rapid $bpy^{-\bullet} \rightarrow MQ^+$ electron transfer occurs following $Os^{II} \rightarrow$ bpy or Re → bpy excitation. MQ^+ was shown to be the lowest acceptor ligand by transient resonance Raman.[14] In *fac*-$[Re(4,4'\text{-}(CO_2Et)_2bpy)(CO)_3(MQ^+)](PF_6)_2$, a $Re^{II}(4,4'\text{-}(CO_2Et)_2bpy^{-\bullet})$ MLCT state is the lowest excited-state based on emission, but electrochemical measurements point to MQ^+ as the better electron acceptor. Application of S^2FTIR TRS measurements to these excited states has revealed: (1) significant changes in metal−ligand back-bonding between the ground and excited state and between MQ^+ and bpy as acceptor ligands, (2) some special characteristics of MQ^+ as the acceptor ligand including the appearance of an intense ΔA band at $\sim$1610

S1089-5639(98)00225-4 CCC: $15.00

cm^{-1}, which appears to be vibronically coupled to the internal charge distribution of the reduced ligand, and (3) further insight on the competition that exists between MQ^+ and 4,4′-$(CO_2Et)_2$bpy as acceptor ligands in *fac*-[Re(4,4′-$(CO_2Et)_2$bpy)$(CO)_3$(MQ^+)]$^{n+}$ ($n = 1, 2$).

Experimental Section

Materials. The preparation and characterization of *cis*-[Os(bpy)$_2$(CO)(4,4-bpy)](PF_6)$_2$, *cis*-[Os(bpy)$_2$(CO)(MQ^+)](PF_6)$_3$, *fac*-[Re(4,4′-$(CO_2Et)_2$bpy)$(CO)_3$(4-Etpy)](PF_6), *fac*-[Re(4,4′-$(CO_2Et)_2$bpy)$(CO)_3$(MQ^+)](PF_6)$_2$, *fac*-[Re(4,4′-$(CH_3)_2$bpy)$(CO)_3$(4-Etpy)](PF_6), and *fac*-[Re(4,4′-$(CH_3)_2$bpy)$(CO)_3$(MQ^+)](PF_6)$_2$ have been described elsewhere.[14d] CH_3CN was spectrograde from Burdick and Jackson laboratories, and 1,2-dichloroethane was distilled from potassium before use.

In the TRIR measurements all salts except *fac*-[Re(4,4′-$(CH_3)_2$bpy)$(CO)_3$(4-Etpy)](PF_6) and *fac*-[Re(4,4′-$(CH_3)_2$bpy)-$(CO)_3$(MQ^+)](PF_6)$_2$ were dissolved in CH_3CN to give an absorbance of ∼0.5 for the ν(CO) band with an optical path of 0.25 mm. For *fac*-[Re(4,4′-$(CH_3)_2$bpy)$(CO)_3$(MQ^+)](PF_6)$_2$, the lifetime in CH_3CN was too short to be measured by the apparatus employed and a nearly saturated solution of 1,2-dichloroethane was used instead. This gave an absorbance of 0.15 with an optical path length of 0.25 mm. The solutions were deoxgenated by bubbling argon for at least 15 min and then transferred to a solution IR cell with a syringe. A flow cell with a syringe pump was used to avoid complications from photochemical decomposition.

Measurements. The experimental setup used for the S^{2}FTIR TRS measurements has been described elsewhere.[7b] A brief summary is given below. Excitation was achieved by using the third harmonic of a Quanta Ray model DCR-1 Nd:YAG laser (10 ns, ∼3 mJ/pulse) and a step-scan Bruker IFS 88 FT-IR spectrometer equipped with a dual-channel, 100-MHz PAD 82 digitizer for data acquisition. The laser and FT-IR spectrometer were synchronized with a Stanford Research model DG535 pulse generator. A photovoltaic mercury cadmium telluride (MCT) detector with a 50-MHz preamplifier (Kolmar Technology) was used for IR detection. A Ge filter was placed on the window of the detector to block visible emission from the sample and the scattered laser light. The low-pass Ge filter (2250 cm^{-1}) also blocked high-energy IR light, and the low-energy cutoff (1250 cm^{-1}) was limited by the CaF_2 windows of the sample cell. With this limited spectral window (1250 cm^{-1}−2250 cm^{-1}), an undersampling ratio of 8 was used to limit the number of data points collected in the step-scan experiments to reduce data collection time. The limited spectral range was also useful in reducing the saturation of the detector by unwanted IR light and in meeting the requirements of a limited dynamic range imposed by the 8-bit digitizer.

The ac coupled output of the preamplifier was further amplified with a Hewlett-Packard model 461A or Stanford Research model SR 445 amplifier and then recorded in channel A of the PAD 82 digitizer. The dc coupled output of the preamplifier was recorded in channel B of the PAD 82 digitizer. The phase spectrum used to transform the ac interferogram collected in channel A was generated from the dc interferogram collected in channel B. The absorbance difference spectrum was calculated by the relation, $\Delta A(\bar{\nu}, t) = -\log[1 + \Delta I(\bar{\nu}, t)/I(\bar{\nu})]$, where $I(\bar{\nu})$ is the intensity of IR light at energy $\bar{\nu}$ before laser excitation and $\Delta I(\bar{\nu}, t)$ is the change in intensity at time t.

Ground-state absorption spectra were acquired on the same spectrometer in the continuous-scan mode with the solvent spectrum subtracted.

Results

Ground-state absorption and TRIR absorption difference spectra were acquired in CH_3CN except for *fac*-[Re(4,4′-$(CH_3)_2$bpy)$(CO)_3$(MQ^+)](PF_6)$_2$ and *fac*-[Re(4,4′-$(CH_3)_2$bpy)$(CO)_3$(4-Etpy)](PF_6)$_2$, which were acquired in 1,2-dichloroethane. The results for the individual complexes are presented below and summarized in Table 1.

***cis*-[Os(bpy)$_2$(CO)(4,4′-bpy)]$^{2+}$.** The ground-state spectrum of *cis*-[Os(bpy)$_2$(CO)(4,4′-bpy)]$^{2+}$ is shown in Figure 1A with solvent bands subtracted. The band at 1968 cm^{-1} is the ν(CO) stretch, and the 1609 cm^{-1} band is a ν(bpy) ring-stretching mode. The broad band centered at 1645 cm^{-1} is, in part, due to waters of hydration in the lattice of the solid sample, possibly with contributions from ν(bpy) or ν(4,4′-bpy) vibrations.

A S^{2}FTIR TR absorbance difference (ΔA) spectrum of *cis*-[Os(bpy)$_2$(CO)(4,4′-bpy)]$^{2+}$ acquired 10 ns after 355-nm laser excitation is shown in Figure 1B. In comparing the spectra in Figure 1A, B, ν(CO) at 1968 cm^{-1} in the ground-state shifts to 2037 cm^{-1} in the MLCT excited state ($\Delta\bar{\nu}(CO) = +69\ cm^{-1}$), eq 1, and the ν(bpy) band at 1609 cm^{-1} shifts to 1618 cm^{-1} in the excited state and increases in intensity by ∼×2. These changes are consistent with formation of an MLCT excited state,

$$cis\text{-}[Os^{II}(bpy)_2(CO)(4,4'\text{-}bpy)]^{2+} \xrightarrow{h\nu} cis\text{-}[Os^{III}(bpy)(bpy^{-\bullet})(CO)(4,4'\text{-}bpy)]^{2+*} \quad (1)$$

The one-electron reduced form, *cis*-[Os^{II}(bpy$^{-\bullet}$)(bpy)(CO)(4,4′-bpy)]$^+$, was generated in situ by reduction of the MLCT excited state by added 10-methylphenothiazine (10-MePTZ) at ∼0.001 M, eq 2. In the resulting TRIR spectrum, Figure 1C, ν(CO) is shifted to 1929 cm^{-1} ($\Delta\bar{\nu}(CO) = -39\ cm^{-1}$).

$$cis\text{-}[Os^{III}(bpy)(bpy^{-\bullet})(CO)(4,4'\text{-}bpy)]^{2+*} + 10\text{-}MePTZ \rightarrow cis\text{-}[Os^{II}(bpy)(bpy^{-\bullet})(CO)(4,4'\text{-}bpy)]^{+} + 10\text{-}MePTZ^{+\bullet} \quad (2)$$

***cis*-[Os(bpy)$_2$(CO)(MQ^+)]$^{3+}$.** The same set of spectra for *cis*-[Os(bpy)$_2$(CO)(MQ^+)]$^{3+}$ acquired under the same conditions are shown in Figure 2. In the excited state, ν(CO) appears at 2056 cm^{-1} ($\Delta\bar{\nu}(CO) = +87\ cm^{-1}$). An intense ΔA band appears at 1610 cm^{-1} which has an integrated ΔA greater than twice that of ν(CO) and completely overwhelms the ΔA of the ν(bpy) bands. The ΔA spectrum is reproducible from sample to sample and the 1610 cm^{-1} feature appears only if MQ^+ is a ligand. The decay kinetics for the band at 1610 cm^{-1} are the same as for ν(CO) at 2037 cm^{-1} and for the recovery of the ground-state bleach at 1969 cm^{-1}. The 1610-cm^{-1} band also appears in *cis*-[Os^{II}(bpy)$_2$(CO)($MQ^\bullet$)]$^{2+}$ formed by reductive quenching, eq 3, as does ν(CO) at 1957 cm^{-1} ($\Delta\bar{\nu}(CO) = -12\ cm^{-1}$).

$$cis\text{-}[Os^{III}(bpy)_2(CO)(MQ^{\bullet})]^{3+*} + 10\text{-}MePTZ \rightarrow cis\text{-}[Os^{II}(bpy)_2(CO)(MQ^{\bullet})]^{2+} + 10\text{-}MePTZ^{+\bullet} \quad (3)$$

***fac*-[Re(4,4′-$(CH_3)_2$bpy)$(CO)_3$(MQ^+)]$^{2+}$ and *fac*-[Re(4,4′-$(CH_3)_2$bpy)$(CO)_3$(4-Etpy)]$^+$.** Spectra for this pair of complexes were acquired in 1,2-dichloroethane because the lifetime of *fac*-[Re(4,4′-$(CH_3)_2$bpy)$(CO)_3$(MQ^+)]$^{2+*}$ is too short in CH_3CN for S^{2}FTIR TRS measurement by our apparatus. Solvent effects on the spectra are slight. Shifts in ν(CO) for *fac*-[Re^{II}(4,4′-$(CH_3)_2$bpy$^{-\bullet}$)$(CO)_3$(4-Etpy)]$^{+*}$ between CH_3CN and 1,2-dichloroethane are only ∼4 cm^{-1}.

TABLE 1: Energies and Assignments for Selected IR Bands (cm^{-1}) in CH$_3$CN

complexes (as PF$_6^-$ salts)	energies (cm^{-1})	assignment	$\Delta\bar{\nu}$ (cm^{-1})^c
cis-[Os$^{\mathrm{II}}$(bpy)$_2$(CO)(4,4′-bpy)]$^{2+}$	1968	ν(CO)	
	1609	ν(bpy)	
cis-[Os$^{\mathrm{III}}$(bpy$^{-\bullet}$)(bpy)(CO)(4,4′-bpy)]$^{2+*}$	2037	ν(CO)	+69
	1618	ν(bpy)	+9
cis-[Os$^{\mathrm{II}}$(bpy$^{-\bullet}$)(bpy)(CO)(4,4′-bpy)]$^{+}$	1929	ν(CO)	−39
cis-[Os$^{\mathrm{II}}$(bpy)$_2$(CO)(MQ$^+$)]$^{3+}$	1969	ν(CO)	
cis-[Os$^{\mathrm{III}}$(bpy)$_2$(CO)(MQ$^\bullet$)]$^{3+*}$	2056	ν(CO)	+87
	1610	ν(MQ$^\bullet$)	
cis-[Os$^{\mathrm{II}}$(bpy)$_2$(CO)(MQ$^\bullet$)]$^{2+}$	1957	ν(CO)	−12
	1610	ν(MQ$^\bullet$)	
fac-[Re$^{\mathrm{I}}$(4,4′-(CH$_3$)$_2$bpy)(CO)$_3$(4-Etpy)]$^{+\ a}$	2034	ν(CO)	
	1932	ν(CO)^b	
fac-[Re$^{\mathrm{II}}$(4,4′-(CH$_3$)$_2$bpy$^{-\bullet}$)(CO)$_3$(4-Etpy)]$^{+*\ a}$	2059	ν(CO)	+25
	2005	ν(CO)	+73
	1961	ν(CO)	+31
fac-[Re$^{\mathrm{I}}$(4,4′-(CH$_3$)$_2$bpy)(CO)$_3$(MQ$^+$)]$^{2+\ a}$	2036	ν(CO)	
	1937	ν(CO)^b	
fac-[Re$^{\mathrm{II}}$(4,4′-(CH$_3$)$_2$bpy)(CO)$_3$(MQ$^\bullet$)]$^{2+\ a}$	2087	ν(CO)	+51
	1987	ν(CO)^b	+50
	1606	ν(MQ$^\bullet$)	
fac-[Re$^{\mathrm{I}}$(4,4′-(CO$_2$Et)$_2$bpy)(CO)$_3$(4-Etpy)]$^{+}$	2038	ν(CO)	
	1935	ν(CO)^b	
	1737	ν(CO$_2$Et)	
fac-[Re$^{\mathrm{II}}$(4,4′-(CO$_2$Et)$_2$bpy$^{-\bullet}$)(CO)$_3$(4-Etpy)]$^{+*}$	2092	ν(CO)	+54
	2023	ν(CO)	+88
	1975	ν(CO)	+41
	1707	ν(CO$_2$Et)	−30
fac-[Re$^{\mathrm{I}}$(4,4′-(CO$_2$Et)$_2$bpy$^{-\bullet}$)(CO)$_3$(4-Etpy)]^{0}	2015	ν(CO)	−23
	1905	ν(CO)^b	−30
	1697	ν(CO$_2$Et)	−40
fac-[Re$^{\mathrm{I}}$(4,4′-(CO$_2$Et)$_2$bpy)(CO)$_3$(MQ$^+$)]$^{2+}$	2039	ν(CO)	
	1939	ν(CO)^b	
	1737	ν(CO$_2$Et)	
fac-[Re$^{\mathrm{II}}$(4,4′-(CO$_2$Et)$_2$bpy$^{-\bullet}$)(CO)$_3$(MQ$^+$)]$^{2+*}$	2090	ν(CO)	+51
	2026	ν(CO)	+87
	1983	ν(CO)	+44
	1707	ν(CO$_2$Et)	−30
fac-[Re$^{\mathrm{I}}$(4,4′-(CO$_2$Et)$_2$bpy)(CO)$_3$(MQ$^\bullet$)]$^{+}$	2032	ν(CO)	−7
	1928	ν(CO)^b	−11
	1608	ν(MQ$^\bullet$)	

[a] In 1,2-dichloroethane. [b] Overlapping bands. [c] $\Delta\bar{\nu}$ is the change in ν(CO), etc., from the ground-state value.

In the ground-state spectra of *fac*-[Re(4,4′-(X)$_2$bpy)(CO)$_3$(4-Etpy)]$^+$ there is a two-band pattern with a narrow band at 2034 cm^{-1} and a broad one at 1932 cm^{-1} for X = CH$_3$.[15] These complexes have pseudo C_{3v} symmetry, and the vibrations are the totally symmetric A$_1$ (2034 cm^{-1}) and doubly degenerate E (1932 cm^{-1}) normal modes. The symmetry is not truly C_{3v}; the E mode is actually an overlapping composite of A′ and A″ modes (in C_s symmetry).

This pattern changes in *fac*-[Re$^{\mathrm{II}}$(4,4′-(CH$_3$)$_2$bpy$^{-\bullet}$)(CO)$_3$(4-Etpy)]$^{+*}$, with bands appearing at 2059, 2005, and 1961 cm^{-1}. In this case, localizaton of the excited electron on 4,4′-(CH$_3$)$_2$-bpy lowers the effective local symmetry to C_s, and bands attributable to separate A′ and A″ modes are observed.

The ground-state spectrum of *fac*-[Re(4,4′-(CH$_3$)$_2$bpy)(CO)$_3$-(MQ$^+$)]$^{2+}$ is similar, with the A$_1$ and E modes appearing at 2036 and 1937 cm^{-1}, respectively. For this complex, the two ν(CO) band pattern is maintained in the excited state, with bands appearing at 2087 cm^{-1} ($\Delta\bar{\nu}$(CO) = +51 cm^{-1}) and 1987 cm^{-1} ($\Delta\bar{\nu}$(CO) = +50 cm^{-1}). An intense band appears at 1606 cm^{-1} in the ΔA spectrum, analogous to the 1610 cm^{-1} band in *cis*-[Os(bpy)$_2$(CO)(MQ$^+$)]$^{3+*}$.

***fac*-[Re(4,4′-(CO$_2$Et)$_2$bpy)(CO)$_3$(MQ$^+$)]$^{2+}$ and *fac*-[Re(4,4′-(CO$_2$Et)$_2$bpy)(CO)$_3$(4-Etpy)]$^+$.** The shifts in ν(CO) between the ground and MLCT excited states for *fac*-[Re(4,4′-(CO$_2$Et)$_2$bpy)(CO)$_3$(MQ$^+$)]$^{2+}$ and *fac*-[Re(4,4′-(CO$_2$Et)$_2$bpy)(CO)$_3$-(4-Etpy)]$^+$ are the same within experimental error (Table 1 and Figures 3 and 4). A shift in ν(C═O) for the ester groups from 1737 to 1707 cm^{-1} ($\Delta\bar{\nu}$(C═O) = −30 cm^{-1}) in the excited state and the absence of the 1610 cm^{-1} ΔA marker band for MQ$^\bullet$ in *fac*-[Re(4,4′-(CO$_2$Et)$_2$bpy)(CO)$_3$(MQ$^+$)]$^{2+}$ show that 4,4′-(CO$_2$Et)$_2$bpy is the acceptor ligand in both cases.

In the one-electron reduced form, *fac*-[Re$^{\mathrm{I}}$(4,4′-(CO$_2$Et)$_2$bpy$^{-\bullet}$)-(CO)$_3$(4-Etpy)]^0, generated in situ by 10-MePTZ reduction, eq 4,

$$\textit{fac}\text{-}[\mathrm{Re^{II}(4,4'\text{-}(CO_2Et)_2bpy^{-\bullet})(CO)_3(4\text{-}Etpy)}]^{+*} + \mathrm{10\text{-}MePTZ} \rightarrow \textit{fac}\text{-}[\mathrm{Re^{I}(4,4'\text{-}(CO_2Et)_2bpy^{-\bullet})(CO)_3(4\text{-}Etpy)}] + \mathrm{10\text{-}MePTZ^{+\bullet}} \quad (4)$$

ν(CO) shifts to 2015 cm^{-1} ($\Delta\bar{\nu}$ = −23 cm^{-1}) and 1905 cm^{-1} ($\Delta\bar{\nu}$ = −30 cm^{-1}), and the ester ν(C═O) shifts to 1697 cm^{-1} ($\Delta\bar{\nu}$(C═O) = −40 cm^{-1}), Figure 3C. In the spectrum of *fac*-[Re$^{\mathrm{I}}$(4,4′-(CO$_2$Et)$_2$bpy)(CO)$_3$(MQ$^\bullet$)]$^+$, also generated by reductive quenching,

$$\textit{fac}\text{-}[\mathrm{Re^{II}(4,4'\text{-}(CO_2Et)_2bpy)(CO)_3(MQ^{\bullet})}]^{2+*} + \mathrm{10\text{-}MePTZ} \rightarrow \textit{fac}\text{-}[\mathrm{Re^{I}(4,4'\text{-}(CO_2Et)_2bpy)(CO)_3(MQ^{\bullet})}]^{+} + \mathrm{10\text{-}MePTZ^{+\bullet}} \quad (5)$$

the shifts are much smaller, with ν(CO) appearing at ~2032

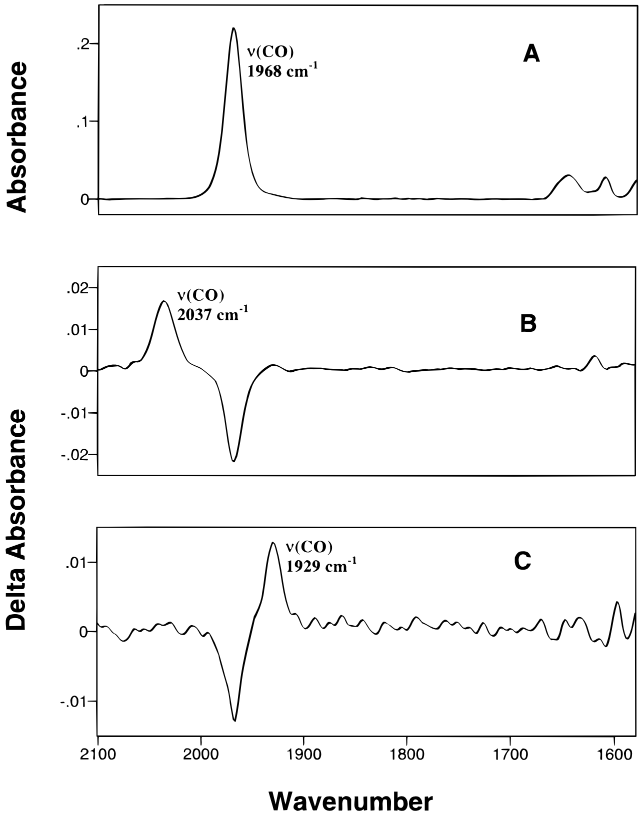

Figure 1. Ground-state spectrum of *cis*-[Os(bpy)$_2$(CO)(4,4′-bpy)]$^{2+}$ (A), S^{2}FTIR TR ΔA spectrum (10 ns after 355-nm laser excitation) (B), and the difference spectrum with 0.002 M added 10-MePTZ (C) 10 ns after 355-nm excitation in CH$_3$CN.

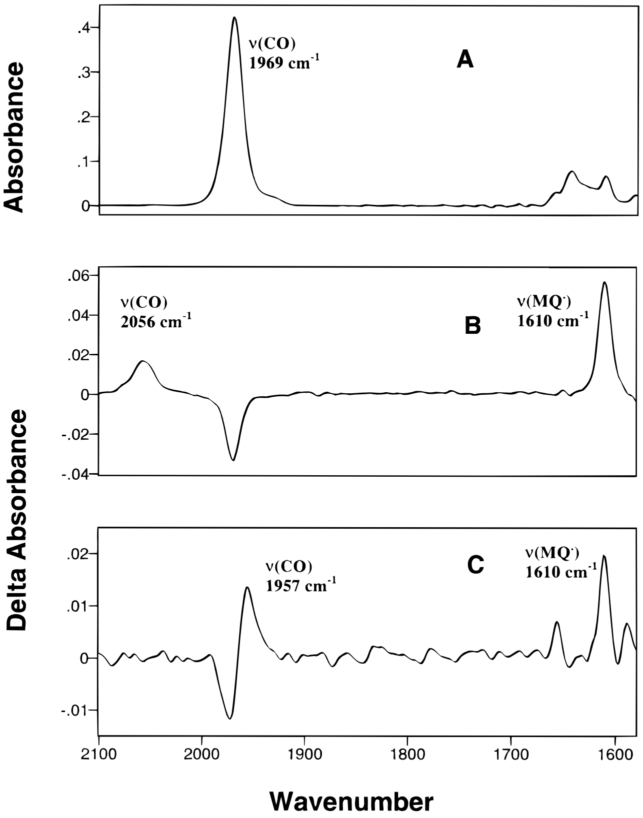

Figure 2. Ground-state FT-IR spectrum of *cis*-[Os(bpy)$_2$(CO)(MQ$^+$)]$^{3+}$ (A), S^{2}FTIR TR ΔA spectrum (10 ns after 355-nm laser excitation) (B), and the difference spectrum with 0.002 M added 10-MePTZ (C) 10 ns after 355-nm excitation in CH$_3$CN.

($\Delta\bar{\nu}$ = <1 cm^{-1}) and 1928 cm^{-1} ($\Delta\bar{\nu} = -11$ cm^{-1}). The added electron is on MQ$^+$ as shown by the intense ΔA ν(MQ$^\bullet$) marker band at 1608 cm^{-1}.

Discussion

Application of S^{2}FTIR TRS to the Os$^{\mathrm{II}}$ and Re$^{\mathrm{I}}$ complexes allows both ν(CO) and ν(bpy) regions to be measured. These results are revealing about three separate issues regarding excited-state electronic structure.

Back-Bonding. Electronic Structure in the Acceptor Ligand. There is a large shift in ν(CO) ($\Delta\bar{\nu}$(CO) = +69 cm^{-1}) in the MLCT excited state of *cis*-[Os(bpy)$_2$(CO)(4,4′-bpy)]$^{2+}$. Comparable shifts occur for [Os(tpy)(bpy)(CO)]$^{2+*}$ (tpy =2,2′:6′,2″-terpyridine) ($\Delta\bar{\nu}$(CO) = +70 cm^{-1}), *cis*-[Os(bpy)$_2$(CO)(py)]$^{2+*}$ ($\Delta\bar{\nu}$(CO) = + 69 cm^{-1}), and [Os(phen)$_2$(CO)Cl]$^{+*}$ ($\Delta\bar{\nu}$(CO) = +73 cm^{-1}).[10] The increase is consistent with partial oxidation at Os, eq 1, and loss of dπ−π*(CO) back-bonding in the excited state. This increases the CO bond order and $\bar{\nu}$(CO).

The opposite occurs upon reduction to *cis*-[Os$^{\mathrm{II}}$(bpy$^{-\bullet}$)(bpy)(CO)(4,4′-bpy)]$^+$ for which $\Delta\bar{\nu}$(CO) = −39 cm^{-1}. Reduction enhances dπ−π*(bpy$^{-\bullet}$) mixing and dπ−π*(CO) back-bonding.

The same trends are observed for the Re$^{\mathrm{I}}$ complexes. Large positive shifts in ν(CO) are observed for the MLCT excited states and smaller negative shifts for the one-electron reduced forms (Table 1). A quantitative understanding of these shifts remains to be developed on the basis of such factors as the energy gap between the ground and excited states, the orbitals occupied, and the extent of orbital mixing with other ligands.

In the mid-IR spectrum of [Os$^{\mathrm{III}}$(bpy)(bpy$^{-\bullet}$)(CO)(4,4′-bpy)]$^{2+*}$, a ground-state ν(bpy) band at 1609 cm^{-1} (ν_{25})[16] shifts to 1618 cm^{-1} and increases in intensity by ~2. Similar changes in ν_{25} have been observed for Ru$^{\mathrm{III}}$(bpy$^{-\bullet}$)(bpy)$_2$]$^{2+*}$ and [Ru$^{\mathrm{III}}$(bpy)$_3$]$^{3+}$.[11] On the basis of normal coordinate analyses of [Ru$^{\mathrm{II}}$(bpy)$_3$]$^{2+}$ and Ru$^{\mathrm{III}}$(bpy$^{-\bullet}$)(bpy)$_2$]$^{2+*}$,[16] the potential energy distribution (PED) in ν_{25} includes 46% ν(C$_2$−C$_3$) and 23% ν(C−N) based on the numbering scheme below. The increase in energy for ν_{25} in the excited state is consistent with decreased back-bonding to the α,α′-diimine fragment of the ligand.[11]

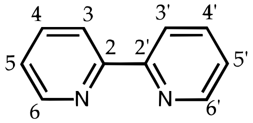

The shift in ν(C=O) for the ester group in *fac*-[Re(4,4′-(CO$_2$Et)$_2$bpy)(CO)$_3$(4-Etpy)]$^+$ between the ground and excited states is −30 cm^{-1}. It is 26 cm^{-1} for [Ru$^{\mathrm{III}}$(4,4′-(CO$_2$Et)$_2$bpy$^{-\bullet}$)(bpy)$_2$]$^{2+*}$. These shifts demonstrate that there is considerable ester character in the acceptor orbital. The fact that only one ν(C=O) band appears in the spectra shows that the excited electron is delocalized over both pyridyl rings, at least on the IR time scale. The shift in *fac*-[Re(4,4′-(CO$_2$Et)$_2$bpy$^{-\bullet}$)(CO)$_3$(4-Etpy)]^0, is −40 cm^{-1}. It is greater because of the loss of the polarization interaction between Re$^{\mathrm{II}}$ and the reduced ligand in the excited state.

MQ$^+$ as an Acceptor Ligand. Following MLCT excitation of *cis*-[Os(bpy)$_2$(CO)(MQ$^+$)]$^{3+}$ or *fac*-[Re(4,4′-(CH$_3$)$_2$bpy)(CO)$_3$(MQ$^+$)]$^{2+}$, the ultimate acceptor ligand is MQ$^+$. This conclusion is based on transient UV−visible, emission, and resonance Raman measurements.[14] The electron-transfer sequence that occurs following Os$^{\mathrm{II}}$ → bpy, Os$^{\mathrm{II}}$ → MQ$^+$ excitation

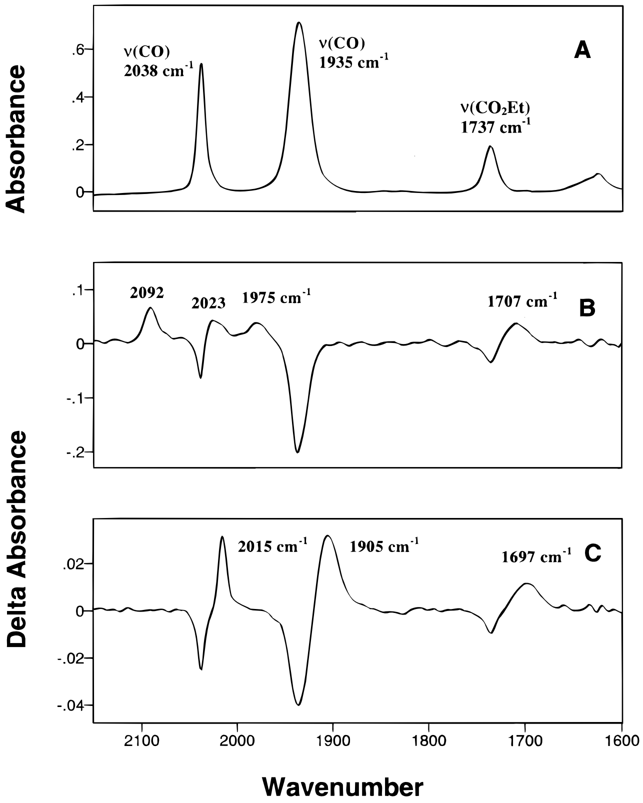

Figure 3. Ground-state spectrum of *fac*-[Re(4,4′-(CO$_2$Et)$_2$bpy)(CO)$_3$-(4-Etpy)]$^+$ (A), S^{2}FTIR TR Δ*A* spectrum (10 ns after 355-nm laser excitation) (B), and the difference spectrum with 0.002 M added 10-MePTZ (C) 10 ns after 355-nm excitation in CH$_3$CN.

SCHEME 1

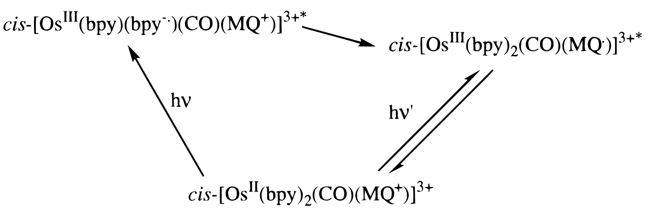

of *cis*-[Os(bpy)$_2$(CO)(MQ$^+$)]$^{3+}$ is illustrated in Scheme 1. A related scheme applies to the Re^{I} analogue.

From the S^{2}FTIR TRS measurements and earlier observations, there are chraracteristic spectroscopic and structural features associated with MQ$^+$ as the acceptor:

(1) The shift in ν(CO) for MQ$^+$ as the acceptor in *cis*-[Os^{III}-(bpy)$_2$(CO)(MQ$^\bullet$)]$^{3+*}$ is +87 cm^{-1}, 18 cm^{-1} greater than for bpy as the acceptor in *cis*-[Os^{III}(bpy$^{-\bullet}$)(bpy)(CO)(4,4′-bpy)]$^{2+*}$ (+69 cm^{-1}). From this it can be concluded that there is greater charge transfer and less dπ−π*(CO) mixing when MQ$^+$ is the acceptor ligand. This is true even though the excited-to-ground-state energy gap for the Os^{III}−MQ$^\bullet$ state (13 300 cm^{-1}) is considerably less than the Os^{III}−bpy$^{-\bullet}$ energy gap (16 800 cm^{-1}).[14a]

(2) The shifts in ν(CO) for the one-electron reduced forms, *cis*-[Os^{II}(bpy)$_2$(CO)(MQ$^\bullet$)]$^{2+}$ and *cis*-[Os^{II}(bpy$^{-\bullet}$)(bpy)(CO)(4,4′-bpy)]$^+$, are −12 and − 39 cm^{-1}, respectively. They are −8, −10 cm^{-1} for *fac*-[Re^{I}(4,4′-(CO$_2$Et)$_2$bpy)(CO)$_3$(MQ$^\bullet$)]$^+$ and −23, −30 cm^{-1} for *fac*-[Re^{I}(4,4′-(CO$_2$Et)$_2$bpy$^{-\bullet}$)(CO)$_3$(4-Etpy)]^0. The greater shifts for 4,4′-(CO$_2$Et)$_2$bpy as the acceptor are consistent with greater dπ−π*(CO) back-bonding induced by dπ−π*(CO$_2$Et)$_2$bpy$^{-\bullet}$ mixing compared to dπ−π*(MQ$^\bullet$) mixing.

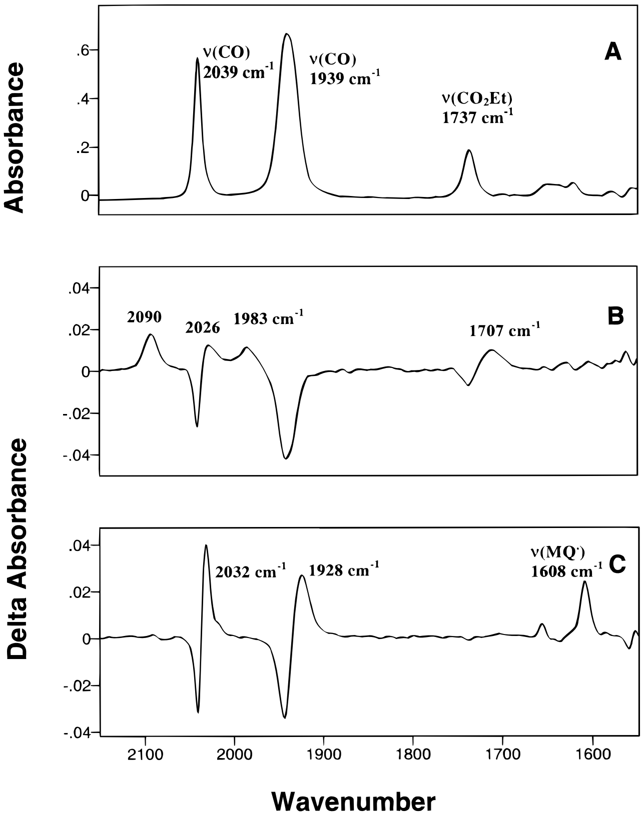

Figure 4. Ground-state spectrum of *fac*-[Re(4,4′-(CO$_2$Et)$_2$bpy)(CO)$_3$-(MQ$^+$)]$^{2+}$ (A), S^{2}FTIR TR Δ*A* spectrum (10 ns after 355-nm laser excitation) (B), and the difference spectrum with 0.002 M added 10-MePTZ (C) 10 ns after 355-nm excitation in CH$_3$CN.

(3) In both *fac*-[Re^{I}(4,4′-(CO$_2$Et)$_2$bpy)(CO)$_3$(MQ$^\bullet$)]$^+$ and *fac*-[Re^{II}(4,4′-(CH$_3$)$_2$bpy)(CO)$_3$(MQ$^\bullet$)]$^{2+*}$, with ν(CO) appearing at 2087 and 1987 cm^{-1}, there are two ν(CO) bands, and the approximately pseudo-C_{3v} local symmetry of the ground state is maintained.

(4) X-ray crystallographic studies have shown that the pyridyl rings of MQ$^+$ in *fac*-[Re(bpy)(CO)$_3$(MQ$^+$)](PF$_6$)$_2$ are noncoplanar, with a ring−ring dihedral angle of $\theta = 47°$.[14a] In the excited state, the rings become coplanar with a decreased py−py inter-ring distance. Coplanarity maximizes electronic delocalization, which overcomes H···H repulsions between the 2, 6 and 2′, 6′ positions of the adjacent rings.

There is less dπ(Os) or dπ(Re) mixing with π*(MQ$^\bullet$) than dπ mixing with π*(bpy) or π*(4,4′-(CO$_2$Et)$_2$bpy) in both the MLCT excited states and one-electron reduced forms. This is, in part, a consequence of the single Re−N binding site for MQ$^+$ compared to the two binding sites for bpy as a ligand. In LCAO constructions of MQ$^\bullet$ or bpy$^{-\bullet}$-based MO's, metal−ligand coupling is dominated by adjacent overlap and dπ−2p-(N) mixing. The degree of metal−ligand π-overlap depends on the amount of 2p character in π*(L). There are two Ru−N bonds for bpy and two dπ−2p(N) overlaps, which enhance mixing.

Local pseudo-C_{3v} electronic symmetry is maintained in *fac*-[Re^{I}(4,4′-(CO$_2$Et)$_2$bpy)(CO)$_3$(MQ$^\bullet$)]$^+$ and in the excited-state *fac*-[Re^{II}(4,4′-(CH$_3$)$_2$bpy)(CO)$_3$(MQ$^\bullet$)]$^{2+*}$. This shows that the local electronic character of MQ$^+$ when it is reduced is comparable to the two pyridyl rings of 4,4′-(CH$_3$)$_2$bpy or 4,4′-(CO$_2$Et)$_2$bpy. This is consistent with electron occupation of a molecular orbital localized largely on the remote pyridinium ring. In a limiting description, the bound pyridyl acts as a bridge between a reduced pyridinium and Re^{I} or Re^{II}

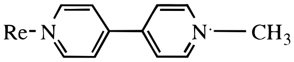

This polarization of electron density away from the bound pyridine also contributes to decreased $d\pi-\pi^*(MQ^\bullet)$ mixing compared to $d\pi-\pi^*(4,4'\text{-}(X)_2bpy)$ mixing.

In the ΔA spectra of *cis*-$[Os^{III}(bpy)_2(CO)(MQ^\bullet)]^{3+*}$, *fac*-$[Re^{II}(4,4'\text{-}(CH_3)_2bpy)(CO)_3(MQ^\bullet)]^{2+*}$, and *fac*-$[Re^{I}(4,4'\text{-}(CO_2Et)_2bpy)(CO)_3(MQ^\bullet)]^+$, $\nu(MQ^\bullet)$ bands of unusual intensity appear at 1606−1610 cm^{-1}. The intensity ratio $\nu(MQ^\bullet)/\nu(CO)$ is ∼2 for the Os complex. The greatly enhanced intensity of this band points to a coupling with changes in internal electronic structure within $MQ^\bullet$ by a non-Condon effect. This mixing of charge-transfer character into a nominally vibrational transition would enhance the IR transition dipole.

Competition between $4,4'\text{-}(CO_2Et)_2bpy$ and MQ^+ as Acceptor Ligand in *fac*-$[Re(4,4'\text{-}(CO_2Et)_2bpy)(CO)_3(MQ^+)]^{n+}$. By comparing $E_{1/2}$ values for the first reductions of *fac*-$[Re^{I}(4,4'\text{-}(CO_2Et)_2bpy)(CO)_3(MQ^+)]^{2+}$ and *fac*-$[Re(4,4'\text{-}(CO_2Et)_2bpy)(CO)_3(4\text{-}Etpy)]^+$, MQ^+ is seen to be a better acceptor ligand than $4,4'\text{-}(CO_2Et)_2bpy$ by 100 mV (CH_3CN, 0.1 M $[N(C_4H_9)_4](PF_6)$).[14] One-electron reduction does give *fac*-$[Re^{I}(4,4'\text{-}(CO_2Et)_2bpy)(CO)_3(MQ^\bullet)]^+$, as evidenced by the appearance of the intense, $\nu(MQ^\bullet)$ marker band at 1608 cm^{-1}, the small shifts in $\nu(CO)$, and the absence of a shift in $\nu(C{=}O)$ for $4,4'\text{-}(CO_2Et)_2bpy$ (Table 1).

The opposite is true in *fac*-$[Re^{II}(4,4'\text{-}(CO_2Et)_2bpy^{-\bullet})(CO)_3(MQ^+)]^{2+*}$, where $4,4'\text{-}(CO_2Et)_2bpy$ is the acceptor on the basis of the shifts in $\nu(C{=}O)$ of -30 cm^{-1}, the absence of the $\nu(MQ^\bullet)$ marker band, and the large shifts in $\nu(CO)$ (Table 1).

The change in ordering from $\pi^*(MQ^+) < \pi^*(4,4'\text{-}(CO_2Et)_2bpy)$ to $\pi^*(MQ^+) > \pi^*(4,4'\text{-}(CO_2Et)_2bpy)$ is another consequence of increased $d\pi(Re^{II}, Re^{I})-\pi^*(4,4'\text{-}(CO_2Et)_2bpy)$ mixing compared to $d\pi(Re^{II}, Re^{I})-\pi^*(MQ^\bullet)$ mixing. In the ground state, $d\pi-2p(N)$ mixing with two N atoms increases back-bonding to $\pi^*(4,4'\text{-}(CO_2Et)_2bpy)$ relative to $\pi^*(MQ^+)$. This increases the energy of $\pi^*(4,4'\text{-}(CO_2Et)_2bpy)$ relative to $\pi^*(MQ^+)$ and contributes to the following ordering: $\pi^*(MQ^+) < \pi^*(4,4'\text{-}(CO_2Et)_2bpy)$.

In the MLCT excited states, Re^{II} is electron-deficient and the polarization interaction between Re^{II} and $\pi^*(MQ^\bullet)$ or $\pi^*(4,4'\text{-}(CO_2Et)_2bpy^{-\bullet})$ becomes important. There is greater $d\pi(Re^{II})-\pi^*(4,4'\text{-}(CO_2Et)_2bpy^{-\bullet})$ mixing because there are two 2p(N) interactions and the electronic polarization within $MQ^\bullet$ is toward the methylated ring. This differential stabilization is sufficient to change the energetically most favorable site of reduction from $\pi^*(MQ^+)$ to $\pi^*(4,4'\text{-}(CO_2Et)_2bpy)$.

Acknowledgment for financial support is made to the Department of Energy under the Grant DEEG02-96ER14607 for T.J.M. and to Buker Optics and the National Science Foundation (Grant DMR-9409107) for R.A.P.

References and Notes

(1) (a) Stoutland, P. O.; Dyer, R. B.; Woodruff, W. H. *Science* **1992**, *257*, 1913. (b) Causgrove, T. P.; Dyer, R. B. *J. Phys. Chem.* **1996**, *100*, 3273.

(2) (a) Walker, G. C.; Hochstraser, R. M. In Laser Techniques in Chemistry, Myers, A. B., Thomas, R. R., Eds.; John Wiley & Sons: New York, 1995; p 385. (b) Owrutsky, J. C.; Li, M.; Locke, B.; Hochstrasser, R. M. *J. Phys. Chem.* **1995**, *99*, 4842.

(3) Heilweil, E. J.; Casassa, M. P.; Cavanagh, R. R.; Stephenson, J. C. *Annu. Rev. Phys. Chem.* **1989**, *40*, 143.

(4) (a) Lian, T.; Bromberg, S. E.; Asplund, M. C.; Yang, H.; Harris, C. B. *J. Phys. Chem.* **1996**, *100*, 11994. (b) Hill, J. R.; Dlott, D. D.; Rella, C. W.; Peterson, K. A.; Decature, S. M.; Boxer, S. G.; Fayer, M. D. *J. Phys. Chem.* **1996**, *100*, 12100.

(5) Weitz, E. *J. Phys. Chem.* **1994**, *98*, 11256.

(6) (a) Turner, J. J.; George, M. W.; Johnson, F. P. A.; Westwell, J. R. *Coord. Chem. Rev.* **1993,** *125*, 101. (b) George, M. W.; Poliakoff, M.; Turner, J. J. *Analyst* **1994,** *119*, 551. (c) George, M. W.; Johnson, F. P. A.; Westwell, J. R.; Hodges, P. M.; Turner, J. J. *J. Chem. Soc., Dalton Trans.* **1993,** 2977.

(7) (a) Chen, P.; Omberg, K. M.; Kavaliunas, D. A.; Treadway, J. A.; Palmer, R. A.; Meyer, T. J. *Inorg. Chem.* **1997**, *36*, 954. (b) Chen, P.; Palmer, R. A. *Appl. Spectrosc.* **1997**, *51*, 580.

(8) (a) Plunkett, S. E.; Chao, J. L.; Tague, T. J.; Palmer, R. A. *Appl. Spectrosc.* **1995**, *49*, 702. (b) Palmer, R. A.; Plunkett, S. E.; Chen, P.; Chao, J. L.; Tague, T. J. *Mikrochim. Acta Suppl.* **1997,** *14*, 603.

(9) Hu, X.; Frei, H.; Spiro, T. G. *Biochem.* **1996**, *35*, 13001.

(10) (a) Schoonover, J. R.; Strouse, G. F.; Dyer, R. B.; Bates, W. D.; Chen, P.; Meyer, T. J. *Inorg. Chem.,* **1996**, *35*, 273. (b) Schoonover, J. R.; Bignozzi, C. A.; Meyer, T. J. *Coord. Chem. Rev.*, in press. (c) Schoonover, J. R.; Strouse, G. F.; Omberg, K. M.; Dyer, R. B.; *Comments Inorg. Chem.* **1995**, *18*, 165.

(11) Omberg, K. M.; Schoonover, J. R.; Treadway, J. A.; Leasure, R. M.; Dyer, R. B.; Meyer, T. J. *J. Am. Chem. Sco.* **1997**, *119*, 7013.

(12) Palmer, R. A.; Chen, P.; Plunkett, S. E.; Chao, J. L. *Mikrochim. Acta Suppl.* **1997**, *14*, 595.

(13) (a) Schoonover, J. R.; Gordon, K. C.; Argazzi, R.; Woodruff, W. H.; Peterson, K. A.; Bignozzi, C. A.; Dyer, R. B.; Meyer, T. J. *J. Am. Chem. Soc.* **1993**, *115*, 10996. (b) Doorn, S. K.; Stoutland, P. O.; Dyer, R. B.; Woodruff, W. H. *J. Am. Chem. Soc.* **1992**, *114*, 3133.

(14) (a) Chen, P.; Curry, M.; Meyer, T. J. *Inorg. Chem.* **1989**, *28*, 2271 (b) Schoonover, J. R.; Chen, P.; Bates, W. D.; Dyer, R. B.; Meyer, T. J. *Inorg. Chem.* **1994**, *33*, 793. (c) Chen, P.; Danielson, E.; Meyer, T. J. *J. Phys. Chem.* **1988**, *92*, 3708. (d) Westmoreland, T. D. Ph.D. Dissertation, University of North Carolina, 1987.

(15) Omberg, K. M.; Schoonover, J. R.; Dyer, R. B.; George, M. W.; Turner, J.; Ishitani, O.; Koike, K.; Chen, P.; Pedersen, L.; Meyer, T. J. manuscript in preparation.

(16) (a) Mallick, P. K.; Danzer, G. D.; Strommen, D. P.; Kincaid, J. R. *J. Phys. Chem.* **1988**, *92*, 5628. (b) Strommen, D. P.; Mallick, P. K.; Danzer, G. D.; Lumpkin, R. S.; Kincaid, J. R. *J. Phys. Chem.* **1990**, *94*, 1357.